Tropomyosin Dynamics in Cardiac Thin Filaments: A Multisite Förster Resonance Energy Transfer and Anisotropy Study

Hui Wang,* Shu Mao,* Joseph M. Chalovich,† and Gerard Marriott*
*Department of Physiology, University of Wisconsin, Madison, Wisconsin 53706; and †Department of Biochemistry and Molecular Biology, Brody School of Medicine at East Carolina University, Greenville, North Carolina 27834

ABSTRACT Cryoelectron microscopy studies have identified distinct locations of tropomyosin (Tm) within the Ca^{2+}-free, Ca^{2+}-saturated, and myosin-S1-saturated states of the thin filament. On the other hand, steady-state Förster resonance energy transfer (FRET) studies using functional, reconstituted thin filaments under physiological conditions of temperature and solvent have failed to detect any movement of Tm upon Ca^{2+} binding. In this investigation, an optimized system for FRET and anisotropy analyses of cardiac tropomyosin (cTm) dynamics was developed that employed a single tethered donor probe within a Tm dimer. Multisite FRET and fluorescence anisotropy analyses showed that S1 binding to Ca^{2+} thin filaments triggered a uniform displacement of cTm toward F-actin but that Ca^{2+} binding alone did not change FRET efficiency, most likely due to thermally driven fluctuations of cTm on the thin filament that decreased the effective separation of the donor probe between the blocked and closed states. Although Ca^{2+} binding to the thin filament did not significantly change FRET efficiency, such a change was demonstrated when the thin filament was partially saturated with S1. FRET was also used to show that stoichiometric binding of S1 to Ca^{2+}-activated thin filaments decreased the amplitude of Tm fluctuations and revealed a strong correlation between the cooperative binding of S1 to the closed state and the movement of cTm.

INTRODUCTION

The two-state steric blocking model (1,2) was the first widely accepted model to explain the molecular regulation of contraction in cardiac and skeletal muscle. This model suggested that calcium binding to troponin triggers an azimuthal movement of tropomyosin (Tm) on the thin filament away from the myosin binding site and although supported by x-ray diffraction studies, it could not explain results obtained from some kinetics studies (3–5). Thus, both theoretical and experimental studies showed that the binding of myosin S1 and the S1-ATPase activity on the regulated thin filament were highly cooperative and that calcium alone did not fully activate the thin filament (6–10). Fluorescence studies using pyrene-labeled Tm (11) and rhodamine-X-labeled S1 (12) generated similar results.

Recently a three-state model has emerged that incorporates key elements of both the steric blocking and kinetic models. In the three-state model, the binding of Ca^{2+} to troponin C (TnC) and the association of myosin with F-actin triggers concerted movements of Tm between the blocked, closed, and open structural states of the thin filament (13). These movements have been mapped by electron microscopy studies of muscle fibers under conditions corresponding to the relaxed (blocked or B-state), Ca^{2+}-activated (closed or C-state), and Ca^{2+}/myosin-activated (open or M-state) states (14–16). These high-resolution studies suggest that a) the blocked state involves an interaction of Tm with a site on the outer domain (subdomain 1) of actin that overlaps with the proposed site of binding of myosin in the strongly bound actomyosin complex; b) the closed state is formed on the binding of Ca^{2+} to TnC and involves an interaction of Tm with a site on inner domain of actin (14,15); and c) the open state is formed upon Ca^{2+}-sensitized binding of myosin to the thin filament and results in a different interaction of Tm on the inner domain of actin (15). An examination of the structures reported by Pirani et al. (16) indicates that the position of the Tm molecule in the blocked and closed states is separated by ~1.5 nm (16).

In principle, Ca^{2+}-mediated movements of Tm between the blocked and closed states and myosin-mediated movements of Tm that generate the open state should be readily detected and quantified using Förster resonance energy transfer (FRET) techniques. Surprisingly though, previous steady-state FRET studies using donor probes at different loci on Tm (Cys-87, Cys-190, Cys-245, Cys-247, and Cys-252) and acceptor probes on F-actin (Gln-41, Lys-61, and Cys-374, as well as the phalloidin and ATP binding sites) have not detected any significant displacement of the Tm molecule on the thin filament in response to Ca^{2+} binding (17–20). A frequency domain fluorescence decay study using Dansyl-Tm and tetramethylrhodamine-phalloidin (TMR-phalloidin) as a FRET pair (19) revealed small differences in the raw phase and modulation data of the donor between the blocked and closed states in filaments containing substoichiometric Tm (19). A model-dependent analysis of these differences generated a best fit that suggested a 17° azimuthal movement of Tm on the thin filament between the low Ca^{2+} and Ca^{2+}-activated states.

Submitted September 1, 2007, and accepted for publication January 15, 2008.

Address reprint requests to Gerard Marriott, Dept. of Physiology, University of Wisconsin, Madison, 1300 University Ave, Madison, WI 53706. Tel.: 608-262-6309; E-mail: marriott@physiology.wisc.edu.

Editor: David D. Thomas.

0006-3495/08/06/4358/12 $2.00

doi: 10.1529/biophysj.107.121129

However, the significance of this result must be balanced by the fact that the small differences in the phase data between the two conditions generated very large uncertainties for the computed angles of $-14° \pm 12°$ and $3° \pm 13°$ for $-Ca^{2+}$ and $+Ca^{2+}$, respectively. In addition, earlier FRET studies used labeling strategies that generated two canonical donor probes per Tm dimer (17–20; as depicted in Fig. 1) that could be separated by as much as 2 nm with respect to a unique site on actin. To overcome the uncertainty in defining the locus of the donor probe in FRET and anisotropy-based analyses of cardiac Tm (cTm) dynamics, we developed a novel labeling approach that introduced a single-tethered donor probe to a unique site on the cTm dimer. The donor probe, positioned at four different loci on the cTm molecule, did not affect the function of cTm and was used in a multi-locus FRET and anisotropy analysis to investigate the effect of Ca^{2+} and S1 binding on the movement of the C-terminus of cTm on the thin filament.

MATERIALS AND METHODS

Cloning, gene expression, and protein purification

The complementary DNA (cDNA) encoding human cTm was amplified by polymerase chain reaction using an adult human heart cDNA library (Invitrogen, Carlsbad, CA) as a template and gene specific primers: 3′-GCGGGATCCATGGACGCCATCAAGAAGAAGATG-5′ and 3′-GCGAAGCTTTTATATGGAAGTCATATCGTTGAGAG-5′. Single cysteine containing mutants of cTm were generated by site-directed mutagenesis and involved replacing the endogenous cysteine with serine (Tm C190S) and substitutions at S206C, T247C, and T282C. The genes were cloned between BamH I and Hind III sites of vector pQE-30 (Qiagen, Valencia, CA), and the vectors were transformed into the M15pRep4 *Escherichia coli* strain. The His-tagged

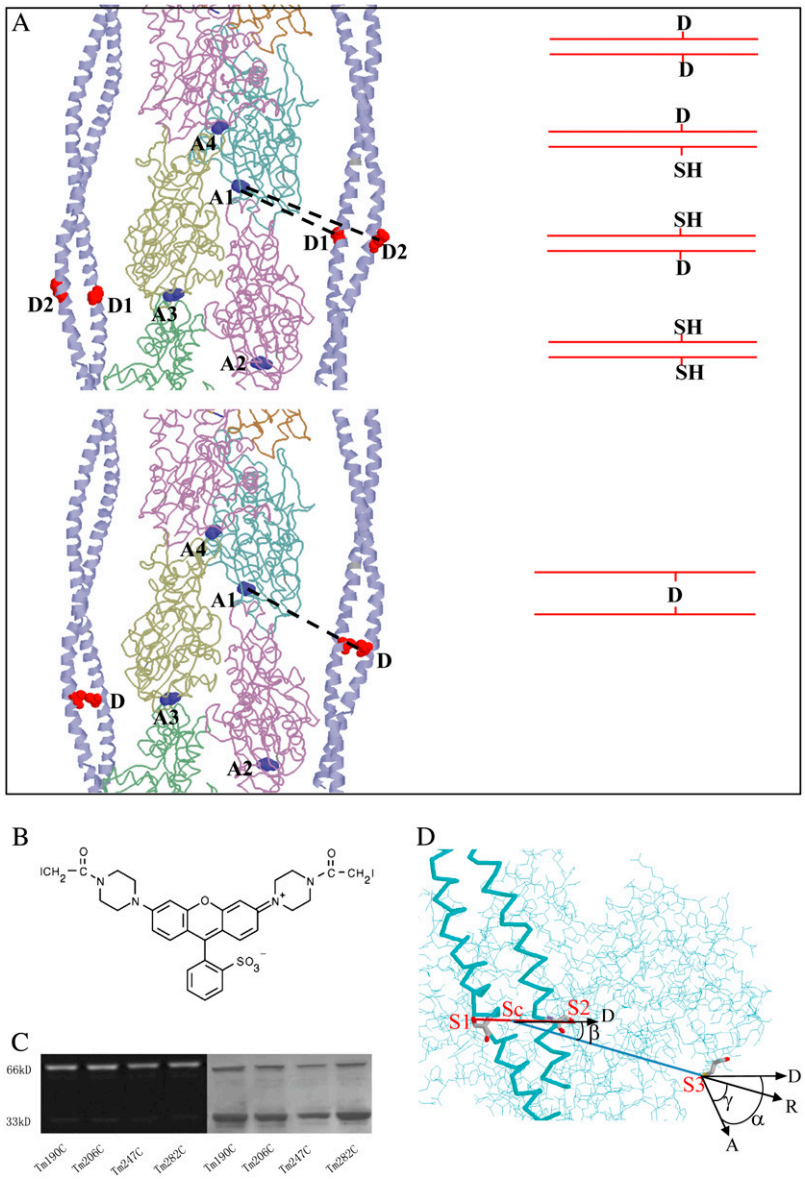

FIGURE 1 Cross-linking of Tm by BSR. (*A*) In earlier FRET studies (17–20), the labeling of Tm with monofunctional probes generated two different donor loci (D_1,D_2) for a single Tm dimer (*upper*). The calculated FRET distance obtained using these preparations, therefore, represented the average weight of the two donor probe loci to the measured value of FRET efficiency. However, BSR-labeled Tm contains a unique and tethered donor locus (D) within a Tm dimer that decreases the uncertainty of FRET measurement compared to earlier FRET studies. The diagrams of molecular models were prepared using Protein Explorer 2.80 (48). (*B*) The chemical structure of BSR. (*C*) SDS-PAGE analysis of BSR conjugates of wild-type cTm and cTm single-cysteine mutants. A twofold molar excess of human cardiac $\alpha\alpha$ Tm and the Tm mutants were labeled with one equivalent of BSR in 0.5 M KCl, 0.05 M Tris, and with pH 8.0 at 37°C for 2 h. The BSR conjugates were analyzed in the SDS-PAGE gel. The fluorescence image (*left*) of BSR-cTm was obtained by exciting the unstained gel using an ultraviolet-plate reader and imaging using a charge-coupled device camera. Protein levels were visualized by staining the same gel with Coomassie blue (*right*) and imaging using white light illumination. (*D*) Schematic diagram of the κ^2 calculation. In the equation $\kappa^2 = (\cos\alpha - 3\cos\beta\cos\gamma)^2$, α is the angle between donor dipole moment (D) and acceptor dipole moment (A), β is the angle between the donor moment and the vector adjoining the centers of the donor and acceptor (R), γ is the angle between the acceptor moment and the adjoining vector. Here, we took the direction of the vector adjoining the two sulfur atoms (S_1 and S_2) of Cys-190 on Tm as the direction of the donor probe (BSR) dipole moment and took the midpoint (S_c) of the two sulfur atoms on Cys-190 of cTm and the sulfur atom (S_3) of Cys-374 of actin as the center of the donor and acceptor (IC5) probes respectively.

proteins were expressed and purified according to the handbook of Ni-NTA affinity chromatography (Qiagen).

Labeling of proteins

G- and F-actin

Actin from chicken skeletal muscle was prepared according to the standard Spudich-Watt protocol (21). G-Actin was stored in G-buffer (5 mM Tris, 0.2 mM ATP, 0.2 mM $CaC1_2$, 1 mM dithiothreitol (DTT), pH 8.0) and used within 3 weeks. The concentration of G-actin was calculated using an extinction coefficient at 290 nm of 0.63 $mg^{-1} \cdot mL \cdot cm^{-1}$ (22). G-Actin was labeled at Cys-374 by using a fivefold excess acceptor probe (IC5-PE-maleimide, Dojindo, Kumaoto, Japan or TMR-maleimide, Invitrogen) in DTT-free G-buffer (5 mM Tris, 0.2 mM $CaCl_2$, 0.1 mM ATP, pH 8.0) at 37°C for 2 h. Unlabeled dye was removed by running the reaction mixture (1 ml) over an Econo-Pac 10DG column (Bio-Rad, Hercules, CA). Labeled actin was converted to F-actin by adding KCl and $MgCl_2$ to 100 mM and 2 mM (F-buffer), respectively, in the presence of a 1.5-fold excess of phalloidin (Sigma, St. Louis, MO) and left overnight on ice in the dark, centrifuged at 85,000 $\times$ *g* for 1 h and resuspended in F-buffer. The labeling ratio was 0.97 for IC5/actin and 0.99 for TMR/actin.

Cardiac tropomyosin

His-tagged cTm (Cys-190) and the three single-cysteine cTm mutants were labeled with bis-((*N*-iodoacetyl)piperazinyl)sulfonerhodamine (BSR; Molecular Probes, Eugene, OR) at a molar ratio of 2:1 in Tm buffer (50 mM Tris, 500 mM KCl, pH 8.0) at 37°C for 2 h. Unconjugated BSR was removed by running the 1 ml reaction mixture over a preequilibrated Econo-Pac 10DG column. The eluted colored proteins were subsequently labeled with a fivefold excess of the quencher probe, QSY9-maleimide (Molecular Probes) at 37° for 2 h. The free QSY9 dye was removed by running the reaction over a separate Econo-Pac 10DG column. cTm mutants were labeled with fivefold excess fluorescein-maleimide in the same condition as above, and free fluorescein was removed by running the reaction over an Econo-Pac 10DG column. The labeling ratio was 0.67 for Tms206C and 0.78 for TmT247C.

Other proteins

Cardiac troponin complex from bovine cardiac muscle was prepared according to Potter (23). Myosin S1 from rabbit skeletal muscle was prepared according to Weeds and Taylor (24).

Characterization of protein conjugates

Labeled proteins were characterized by using absorption spectroscopy, sodium dodecylsulfate-polyacrylamide gel electrophoresis (SDS-PAGE), and fluorescence imaging of labeled proteins within the gel. The molar extinction coefficient for IC5 was taken as 150,000 $M^{-1} \cdot cm^{-1}$ (G. Marriott, unpublished result), whereas BSR, TMR, fluorescein, and QSY9 were taken as 88,000 $M^{-1} \cdot cm^{-1}$, 95,000 $M^{-1} \cdot cm^{-1}$, 83,000 $M^{-1} \cdot cm^{-1}$, and 90,000 $M^{-1} \cdot cm^{-1}$, respectively (Invitrogen).

Reconstitution of thin filaments

Thin filaments were reconstituted with purified donor-labeled cTm, acceptor-labeled or unlabeled F-actin, and/or troponin. The mixture was incubated on ice overnight and centrifuged at 85,000 $\times$ *g* for an hour. The stoichiometry of actin/cTm/troponin was determined by SDS-PAGE analyses and found to be 7:1:1. The pellet was resuspended in appropriate buffers (the buffer for ATPase measurement with Ca^{2+} and without Ca^{2+}, and the buffer for fluorescence measurement with Ca^{2+} and without Ca^{2+}).

Spectroscopic measurements

The absorption spectra of free and labeled proteins were recorded with a Shimadzu PC1601 spectrophotometer (Shimadzu, Columbia, MD). Fluorescence emission spectra of BSR-$(cTm)_2$ within donor only and donor-acceptor labeled reconstituted thin filament complexes were measured at 25°C using an SLM-AB2 fluorimeter according to Heidecker et al. (25). The excitation and emission wavelengths were set at 540 nm and between 560 and 750 nm (both with 4 nm band pass) for the BSR-IC5 FRET pair or at 490 nm and between 500 and 650 nm for the fluorescein-TMR FRET pair. Steady-state emission spectra (4 nm band pass) were measured using magic angle excitation and corrected for the detection response of the instrument (26).

Anisotropy measurements

Steady-state anisotropy values of BSR conjugates of cTm and cTm mutants were measured using a T-format configuration using an SLM-AB2 fluorometer according to Marriott and colleagues (26). The excitation and emission wavelengths were set to 510 nm and 580 nm (both with 8 nm band pass), respectively. The anisotropy value was calculated from 20 s recordings of the four orientations of the excitation and emission polarizers (26). Anisotropy measurements were calibrated using the SLM-AB2 by measuring TMR in 99% glycerol ($r = 0.390 \pm 0.007$) and TMR in methanol ($r = 0.012 \pm 0.004$).

ATPase activity assays

The S1-ATPase in relaxed and Ca^{2+}-activated thin filaments reconstituted with wild-type cTm mutants and their fluorescently labeled conjugates was measured using the malachite green inorganic phosphate assay at 25°C in 10 mM MOPS (3-(*N*-morpholino)propanesulfonic acid), 3 mM $MgCl_2$ and 1 mM ATP, with 0.1 mM $CaCl_2$ or 1 mM EGTA ($-Ca^{2+}$), pH 7.0, according to Kodama and colleagues (27).

Analysis of molecular proximity using FRET data

The corrected fluorescence emission spectra of wild-type cTm and single-cysteine mutants of cTm reconstituted within functional thin filaments were recorded in the absence and presence of the fluorescent acceptor, IC5, attached to Cys-374 on actin. The efficiency of FRET was computed by

$$E_T = \left(1 - \frac{F_{DA}}{F_D}\right)\frac{1}{f_a},$$

where F_{DA} and F_D are the integral of the intensities of the BSR fluorescence from 560 nm to 610 nm in the presence and absence of IC5, and f_a is the fraction of IC5 labeling.

Förster (28) derived the rate of energy transfer between a donor and acceptor, given by

$$k_T = \frac{\phi_D \kappa^2}{\tau_D R^6}\left[\frac{9000(\ln 10)}{128\pi^5 N n^4}\right]\int_0^\infty F_D(\lambda)\varepsilon_A(\lambda)\lambda^4 d\lambda,$$

where k_T is the rate of energy transfer, τ_D is the fluorescence lifetime of the donor, κ^2 is the orientation factor between the fluorophores, n is the refractive index of the medium, ϕ_D is the quantum yield of the donor, ε_A is the molar absorptivity of the acceptor, and R is the distance in angstroms between the donor and acceptor molecules. The efficiency of FRET can be computed using the relationship

$$E_T = \frac{k_T}{\tau_D^{-1} + k_T}.$$

Calculation of transfer efficiency is based on the assumption that every cross-linked BSR probe bound to cTm in the filament is capable of undergoing

energy transfer with IC5-labeled actin protomers in the filament. Spectroscopic characterization of the labeling ratios of BSR to IC5 and actin within reconstituted thin filaments showed that this condition was satisfied. The angular dependence of the dipole-dipole energy transfer, the κ^2 value, is given by

$$\kappa^2 = (\cos\alpha - 3\cos\beta\cos\gamma)^2,$$

where α is the angle between the donor and acceptor transition moments, β is the angle between the donor moment and the line adjoining the centers of the donor and acceptor, and γ is the angle between the acceptor moment and the line joining the centers of the donor and acceptor (as shown in Fig. 1 *D* (29)). Although the donor was tethered and fixed to cTm, the Cy5-acceptor fluorophore, attached to actin by means of a long and flexible linker $[-(CH_2)_5-]$, exhibited considerable rotational freedom (shown later). The validity of assuming a value for the orientation factor (κ^2) of 2/3 (described in Results and Discussion) is based on a detailed analysis of available structural data and anisotropy measurements of our experimental system as well as previous arguments (25). The refractive index was taken as 1.33 (29). The quantum yield of BSR-labeled thin filaments (0.147) was determined by comparing the corrected, integrated emission spectrum of the labeled filaments with the corrected, integrated emission spectrum of Rhodamine 101 in ethanol, using a quantum yield of 1.0 (30), with the same optical density at the excited wavelength used in the emission measurement (540 nm). The value of the spectral overlap integral $J(\lambda)$ was calculated using the expression

$$J(\lambda) = \frac{\int_0^\infty F_D(\lambda)\varepsilon(\lambda)\lambda^4 d\lambda}{\int_0^\infty F_D(\lambda)d\lambda}$$

using the corrected and normalized emission spectrum of labeled filaments; $\varepsilon(\lambda)$, the molar absorptivity of IC5-labeled actin as a function of wavelength, is based on a value at 650 nm of 150,000 $M^{-1} \cdot cm^{-1}$.

RESULTS AND DISCUSSION

A new labeling approach for FRET-based studies of tropomyosin dynamics

Previous FRET-based analyses of the functional dynamics of Tm within thin filaments employed Tm conjugates labeled with donor probes at substoichiometric levels (17–20). Since the functional form of Tm is a coiled-coil dimer (illustrated in Fig. 1), FRET may arise from two different donor loci. Furthermore, unless steps are taken to maintain a low donor/Tm labeling ratio, these preparations will contain a population of Tm dimers harboring two donor probes. As schematized in Fig. 1, FRET analyses using heterogeneously labeled donor probes on Tm reflect the average weight of transfer events for the two donor loci, which reduces the precision of the distance measurement. Although the separation between the sulfur atoms of the two Cys-190 residues in the Tm dimer is only 0.4 nm (31), the size of the donor probe (~1 nm) and the type of linkage group (maleimido, caproate, ethylenediamino) can increase the distance between the two donor loci by more than 2.0 nm, i.e., longer than the proposed Ca^{2+}-induced movement of Tm (16). This potential problem was eliminated in this study by labeling Tm with a homobifunctional rhodamine probe (BSR), which cross-links the in-register cysteine residues in cTm to generate a single tethered donor probe per cTm dimer. We note, as an aside, that this labeling strategy would also be applicable to the larger number of natural and engineered homodimeric proteins harboring in-register cysteine residues, e.g., leucine zippers and LIM proteins (32,33).

As shown in Fig. 2 *A*, substoichiometric labeling of cTm with BSR can generate three Tm species: the BSR cross-linked within the cTm dimer, BSR probe attached to only one cysteine residue in the cTm dimer, and unlabeled cTm. Several reaction parameters were optimized to increase the yield of BSR cross-linked cTm dimers, including temperature, labeling time, and the BSR/cTm ratio. The condition that generated the highest yield (~20%) of BSR cross-linked cTm dimer (Fig. 1 *C*) required mixing 30 μM cTm and 15 μM BSR, rapidly delivered from a 10 mM stock solution in DMF, in 0.5 M KCl, 0.05 M Tris, with pH 8.0 at 37° for 2 h. The distribution of BSR fluorescence within labeled Tm using the optimized cTm reaction, as imaged from an unstained SDS-PAGE gel, showed that cTm dimer contained most of the fluorescence with a small percentage present in the cTm monomer band, even though the Coomassie staining of the same gel showed that most of the cTm was monomeric. We conclude from this study that the labeling of one Cys-190 in the cTm dimer facilitates the cross-linking to the second in-register Cys-190 residue.

Attempts made to separate BSR-cross-linked cTm dimer from the small amount of monomeric BSR-labeled cTm were unsuccessful, e.g., by using gel filtration in 8 M urea or extraction of the dimer from SDS-PAGE. Rather, a novel approach was developed to isolate the fluorescence emission from BSR-cross-linked cTm from non-cross-linked BSR-cTm conjugates by subsequent labeling of unreacted Cys-190 residues with an excess of QSY-9-maleimide. This strategy effectively quenched BSR emission from non-cross-linked cTm but did not affect fluorescence in the BSR-cross-linked dimer. The effectiveness of this QSY-9 quenching approach was evaluated in a comparative study in which the fluorescence emission of identical concentrations of cTm substoichiometric labeled with monoreactive TMR-maleimide was measured without, or after labeling with, QSY-9-maleimide. As can be seen in Fig. 2 *C* (*upper*), the robust fluorescence of TMR in the singly labeled TMR-cTm preparation was quenched by more than 99% after labeling other Cys-190 residues in the preparation with QSY-9-maleimide, i.e., QSY9 effectively eliminated the fluorescence signal from TMR in the cTm conjugate. On the basis of these studies, the labeling condition was modified to include a posttreatment of the cTm-BSR mixture with a fivefold excess of QSY-9 maleimide for 2 h. Free BSR or QSY9-mal was removed from cTm conjugates by using PD-10 chromatography.

Quantitative analysis of the fluorescence within BSR and BSR/QSY9-labeled cTm showed that QSY9 quenched only 5% of the BSR-cTm signal (Fig. 2 *C*, *lower*); this result suggested that using the labeling conditions detailed earlier, 95% of the cTm dimer was cross-linked with BSR, and the

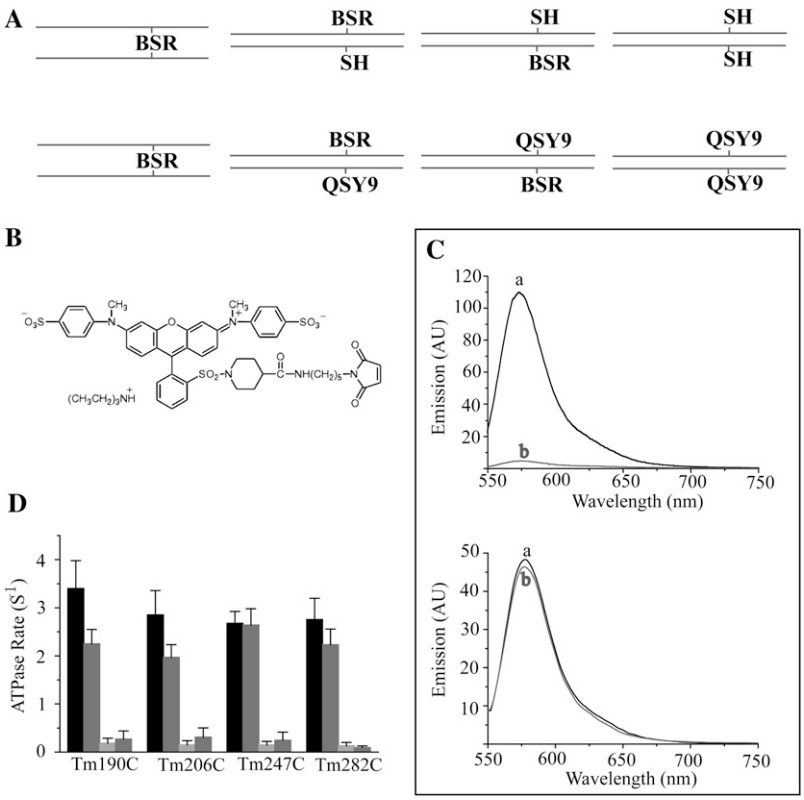

FIGURE 2 Effect of QSY9 on the fluorescence emission of BSR-labeled Tm. (*A*) Schematic representation of the populations of Tm dimer generated with a substoichiometric level of BSR (*top*). Expected populations obtained after labeling of the sample shown in *A* with an excess of QSY9-maleimide (*bottom*). (*B*) The structure of QSY9-malaimide. (*C*) Upper panel: (*a*) Fluorescence emission spectra of cTm (Cys-190) labeled with a substochiometric level of monofunctional TMR-maleimide. (*b*) Same preparation shown in *a* after labeling with QSY9-maleimide, which quenches the fluorescence of TMR molecules within the same dimer by more than 99%. Lower panel: (*a*) Fluorescence spectrum of a TMR-labeled cTm preparation. (*b*) Same sample as shown in *a* after gently mixing a fivefold excess of a cTm preparation stoichiometrically labeled with QSY9. The TMR emission is quenched by <5% upon mixing QSY9-cTm showing that the labeled cTm dimer does not undergo significant rates of dissociation and exchange. (*D*) Activity of the Ca^{2+}-regulated S1 ATPase within thin filaments reconstituted with wild-type cTm, cTm mutants, and their conjugates. Labeled and unlabeled human $\alpha\alpha$-Tm and Tm mutants were reconstituted into thin filaments as described in Materials and Methods. S1 was added to the wild-type and mutant preparations shown in the figure, and their ATPase activities were measured at 25°C in 10 mM MOPS (pH = 7), 3 mM $MgCl_2$, and 1 mM ATP, with 0.1 mM $CaCl_2$ ($+Ca^{2+}$) or 1 mM EGTA ($-Ca^{2+}$). Protein concentrations were 5 μM F-actin, 0.71 μM cTm, 0.71 μM troponin, and 0.1 μM S1. The free phosphate concentration was determined using the malachite green method. The plot shows the ATPase rate on the *y* axis ($n = 3$) for the four Tm conjugates (i.e., cTm190C, cTm206C, cTm247C, and cTm282C). The columns from left to right represent the following conditions: unlabeled Tm with Ca^{2+}, BSR/Qsy9-labeled Tm with Ca^{2+}, unlabeled Tm minus Ca^{2+}, and BSR/QSY9-labeled Tm minus Ca^{2+}.

remainder of the BSR emission within non-cross-linked cTm was quenched by QSY9. The integrated fluorescence emission from cross-linked BSR within each of the other three cTm mutants, i.e., Cys-206, Cys-247, and Cys-282, was also quenched by 5% or less after reaction using an excess of QSY9 (data not shown).

Spectroscopic characterization of cTm conjugates

Absorption spectroscopy along with independent measurements of cTm protein content was used to quantify the ratio of BSR, cTm, and QSY9 within cTm conjugates. The labeling ratios determined for the different single-cysteine cTm mutants were 1), Cys-190; 0.23 for BSR-cTm and 1.54 for QSY9-cTm; 2), Cys-206; 0.21 for BSR-cTm and 1.60 for QSY9-cTm; 3), Cys-247; 0.21 for BSR-cTm and 1.62 for QSY9-cTm; and 4), Cys-282; 0.19 for BSR-cTm and 1.67 for QSY9-cTm.

Functional characterization of cardiac tropomyosin conjugates

Measurements of myosin-S1 ATPase in the relaxed and Ca^{2+}-activated reconstituted thin filaments were conducted by using a modified malachite green assay for inorganic phosphate according to Kodama et al. (27). In all cases, the S1-ATPase activity increased more than eightfold for reconstituted filaments composed of either unlabeled or BSR cross-linked cTm (wild-type or single-cysteine mutants) as summarized in Fig. 2 *D*. On the basis of these results, it could be argued that cross-linking of cTm by BSR does not affect the ability of the conjugate to regulate the S1-ATPase within reconstituted thin filaments. Further, structural fluctuations would be restrained in the vicinity of the cross-link; so it could be argued that extensive folding-unfolding transitions within the region of the cross-link are not critical for the regulation of thin filaments.

FRET between BSR-tropomyosin and IC5-actin

The relative fluorescence quantum yield of BSR-cTm within the four cTm mutants that were stoichiometrically bound to F-actin stabilized with unlabeled phalloidin was determined according to a previous study from this group (25). FRET efficiencies were measured for BSR attached to the four different sites on cTm and IC5 stoichiometrically labeled to Cys-374 on F-actin (see Table 2 and Fig. 3). Applying the following measured values and constants to the Förster equation (BSR lifetime of 4 ns; quantum yield of 0.147; $n = 1.33$; $\kappa^2 = 2/3$; $J = 6.33 \times 10^{15}$ M^{-1} cm^{-1} nm^4; extinction coefficient for IC5 of 150,000 $M^{-1}cm^{-1}$) yielded a value of 4.90 nm for the R_0 between the BSR and IC5 FRET pair on F-actin.

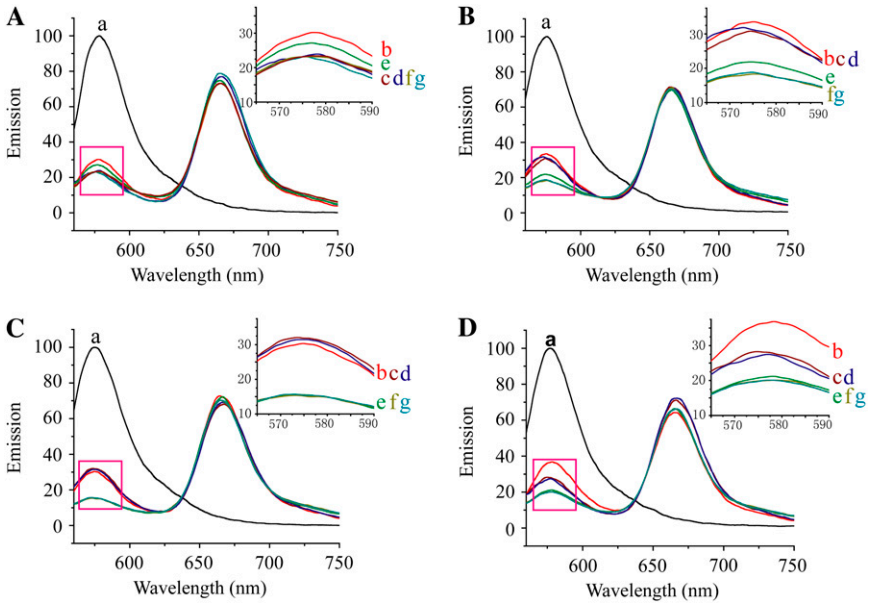

FIGURE 3 Emission spectra of BSR-labeled Tm and Tm mutants in thin filaments in the presence and absence of IC5. BSR-cTm mutants were reconstituted within functional thin filaments harboring either IC5-labeled F-actin (at Cys-374) or unlabeled F-actin, as described in Materials and Methods. Emission spectra were recorded at 25°C. The excitation wavelength was 540 nm and emission collected from 550 nm to 750 nm. Protein concentrations were 5 μM F-actin, 0.71 μM Tm, 0.71 μM troponin, and 5 μM S1. (*A*) Wild-type Tm, (*B*) TmS206C, (*C*) TmT247C, and (*D*) TmT282C, where (*a*) Tm-BSR/F-actin, (*b*) Tm-BSR/F-actin-IC5, (*c*) Tm-BSR/F-actin-IC5/Tn/+Ca^{2+}, (*d*) Tm-BSR/F-actin-IC5/Tn/-Ca^{2+}, (*e*) Tm-BSR/F-actin-IC5/S1, (*f*) Tm-BSR/F-actin-IC5/Tn/S1/+Ca^{2+}, and (*g*) Tm-BSR/F-actin-IC5/Tn/S1/-Ca^{2+}.

κ^2

The only unknown variable in the Förster equation is the orientation factor, κ^2, which is related to the directions of the emission and absorption dipole moments of the donor and acceptor probes according to

$$\kappa^2 = (\cos\alpha - 3\cos\beta\cos\gamma)^2,$$

where α is the angle between the donor and acceptor dipole moments, β is the angle between the donor moment and the line connecting the centers of the donor and acceptor, and γ is the angle between the acceptor moment and the line connecting the centers of the donor and acceptor (as shown in Fig. 1 *d*, (29)). The average of κ^2 is 2/3 if the orientation of both the donor and acceptor is random. The difference between this commonly assumed, spatially averaged value of κ^2 (17–20,25,35) and the actual value can lead to an error in the distance between the FRET pair, although this is no larger than 35% (34). Rigorous validation of this assumption is rarely provided, even in cases when at least one probe is known to be immobile (17–20). The effect of the κ^2 assumption on the distance measurements was evaluated in this study using data from available structures and anisotropy measurements. The anisotropy value for IC5-PE-maleimide labeled to Cys-374 of actin in filaments—where only 9% of the protomers contain the acceptor probe, i.e., in the absence of homo-FRET (25)—was 0.18 ± 0.01 (compared to the r_o value of 0.39 ± 0.01 for IC5 in 99% glycerol), suggesting the probe experiences local motions. On the other hand, the high anisotropy value of BSR cross-linked cTm recorded within the thin filament, as shown in Table 4, suggested that the donor probe could only undergo orthogonal movements dictated by the entire cTm molecule, as discussed later. To test whether using 2/3 is still valid in this study, we estimated the κ^2 value according to Dale and Eisinger (35,36):

$$\langle\kappa^2\rangle = \frac{1}{3}(1 + 3\cos^2\theta).$$

This analysis can be applied to systems in which one dye is fixed and the other one has a random orientation. Thus θ is the angle between the dipole moment of the fixed dye and the line connecting the centers of the donor and acceptor, which is β in our study. We used a published model of the thin filament (16) to calculate the angle β. The C-terminus of Tm is missing in this model; so we appended and aligned a curved Tm model by Holmes to generate the coordinates of the sulfur atoms of Cys-190 on Tm (S_1 and S_2) and that of Cys-374 on actin (S_3), as shown in Fig. 1 *D*. Thus, the dipole moment of BSR was approximately parallel to the vector from S_1 to S_2, and we assumed the midpoint of S_1 and S_2 was the center of the donor (BSR) dipole moment (25), whose coordinate was $S_c = (S_1 + S_2)/2$. The coordinate of the acceptor probe (IC5) was assumed to a first approximation as the sulfur atom on Cys-374 of actin (S_3). The distance between S_c and S_2 is given by

$$d_{c2} = \sqrt{\sum_{i=x,y,z}(S_{ci} - S_{1i})^2}.$$

The distances between S_c and S_3 (d_{c3}), and the distance between S_2 to S_3 (d_{23}) can be calculated in the same way. Using trigonometry, β can be calculated as

$$\cos\beta = \frac{d_{23}^2 - d_{c2}^2 - d_{c3}^2}{2d_{c2}d_{c3}}.$$

The calculated angle β is shown in Table 1. The value of $\langle\kappa^2\rangle$ from the donor to the nearest acceptor was 0.70 in the absence of Ca^{2+} and 0.45 in the presence of Ca^{2+}. The error in the subsequent calculation of distance using these computed values of $\langle\kappa^2\rangle$, compared to the assumption using 2/3, was <6% in both cases. The difference in the value of

TABLE 1 Orientation of BSR labeled on wild-type cTm to Cys-374 on actin determined from the thin filament model (16) and its effect on the calculation of the donor-acceptor distance

	$+Ca^{2+}$				$-Ca^{2+}$				
	R(Å)	$\cos^2\theta$	$\langle\kappa^2\rangle$	$R_{0C}/R_{0(2/3)}$	R(Å)	$\cos^2\theta$	$\langle\kappa^2\rangle$	$R_{0C}/R_{0(2/3)}$	$R_{0C}(+Ca)/R_{0C}(-Ca)$
A1	43.7	0.12	0.45	0.94	35.0	0.37	0.70	1.01	0.93
A2	56.0	0.01	0.34	0.90	51.4	0.00	0.33	0.89	1.01
A3	57.9	0.61	0.94	1.06	62.0	0.69	1.02	1.07	0.99
A4	59.5	0.85	1.18	1.10	64.5	0.90	1.23	1.11	0.99

R_{0C} is the Förster distance computed using the computed $\langle\kappa^2\rangle$ values, which were calculated by using the thin filament model (16), and $R_{0(2/3)}$ is the Förster distance by assuming $\langle\kappa^2\rangle$ is 2/3.

$\langle\kappa^2\rangle$ in response to an orthogonal movement of Tm upon Ca^{2+} binding to the thin filament resulted in a difference of R_0 of only 7%.

In this calculation, we used the thin filament model from Pirani et al. (16), which reported a relatively large movement of Tm upon Ca^{2+} binding (~25° azimuthal movement), whereas an x-ray fiber diagram revealed only an ~15° movement (37), which if accurate would result in an even smaller $\langle\kappa^2\rangle$. A similar conclusion was reached in considering the effect of different values of $\langle\kappa^2\rangle$ between the BSR donor to other acceptor probes on F-actin (Table 1). Importantly though, even without knowing the exact value of β, since the value for $\cos^2\beta$ has a maximum of 1 and minimum of 0, the corresponding values of $\langle\kappa^2\rangle$ will have a maximum of 1.33 and a minimum of 0.33, which can result in a maximal error of 12% in the distance calculation. Finally, we considered findings from a recent study by VanBeek et al. (38), who showed that the inflexibility of a probe linked via maleimide chemistry could result in a high correlation between the angular orientation and spatial position of the probe. In our study, however, the longer linker between the maleimide and the fluorophore (IC5-PE-Mal) did not constrain the flexibility of the probe, as seen from the anisotropy value ($r = 0.18$); so there should be little correlation between $\langle\kappa^2\rangle$ and the Förster distance. Further evidence against the association discovered by Vanbeek et al. (38) may be deduced from our previous studies (25,39), where the value of $\langle\kappa^2\rangle$ was experimentally determined using microscope-based anisotropy measurements of probes on single actin filaments. These determinations were possible only because the dipole moment of the probe was fixed and highly ordered on the filament and generated anisotropy values on a single filament that exceeded the Perrin limit of 0.5 (39). On the other hand, the relatively low anisotropy value measured for IC5-PE on F-actin suggested that acceptor probes on the filament were disordered.

Multisite FRET analysis of proximity between sites on tropomyosin and F-actin

Unregulated filaments: BSR-(cTm)$_2$-F-actin

Measurements of FRET efficiency between BSR, attached to sites on the C-terminal half of cTm (Cys-190, Cys-206, Cys-247, and Cys-282), and IC5-actin (Cys-374) within unregulated filaments (i.e., cTm-F-actin in the absence of troponin) are summarized in Table 2. These values were used to calculate molecular proximity using the Förster equation (Materials and Methods). The calculated distances between the loci on cTm and actin were as follows: cTm (Cys-190) to actin, 4.40 ± 0.13 nm; cTm (Cys-206) to actin, 4.21 ± 0.08 nm; cTm (Cys-247) to actin, 4.38 nm ± 0.13 nm; and cTm (Cys-282) to actin, 4.67 ± 0.10 nm (Table 3).

FRET was assumed to occur between the single BSR donor in a cross-linked cTm dimer and the average locus of four potential acceptor probes on F-actin (i.e., acceptor probes on actin that fall within $2R_o$) based on Pirani's thin filament model (16). This is a necessary assumption since the contribution from a specific acceptor probe to the measured FRET efficiency was unknown. Despite this limitation, the multi-FRET studies reported here provided strong evidence to support the view that specific binding events to the thin filament can affect the average FRET efficiency between the BSR and IC5 probes. For example, in the case of unregulated filaments, FRET efficiency was higher for the Cys-206 cTm

TABLE 2 FRET efficiency between BSR-labeled wild-type cTm and cTm single-cysteine mutants and IC5 labeled to Cys-374 on actin ($n = 3$)

	Tm190C	TmS206C	TmT247C	TmT282C
F-actin/Tm	0.66 ± 0.04	0.72 ± 0.02	0.67 ± 0.04	0.58 ± 0.03
F-actin/Tm/Tn($+Ca^{2+}$)	0.72 ± 0.04	0.75 ± 0.03	0.65 ± 0.04	0.67 ± 0.04
F-actin/Tm/Tn($-Ca^{2+}$)	0.75 ± 0.05	0.74 ± 0.03	0.65 ± 0.04	0.68 ± 0.04
F-actin/Tm/S1	0.71 ± 0.03	0.80 ± 0.03	0.76 ± 0.07	0.75 ± 0.06
F-actin/Tm/Tn/S1($+Ca^{2+}$)	0.75 ± 0.03	0.82 ± 0.04	0.76 ± 0.06	0.76 ± 0.03
F-actin/Tm/Tn/S1($-Ca^{2+}$)	0.76 ± 0.04	0.82 ± 0.04	0.76 ± 0.06	0.76 ± 0.04

TABLE 3 Calculated distances between BSR-labeled wild-type cTm and cTm single-cysteine mutants and IC5 labeled to Cys-374 on actin (Å)

	Tm190C	TmS206C	TmT247C	TmT282C
F-actin/Tm	44.0 ± 1.3	42.1 ± 0.8	43.8 ± 1.3	46.7 ± 1.0
F-actin/Tm/Tn(+Ca^{2+})	42.0 ± 1.4	41.2 ± 1.0	44.5 ± 1.2	43.8 ± 1.3
F-actin/Tm/Tn(−Ca^{2+})	41.0 ± 1.7	41.5 ± 1.1	44.5 ± 1.2	43.5 ± 1.4
F-actin/Tm/S1	42.5 ± 1.2	39.2 ± 1.2	40.5 ± 2.7	41.0 ± 2.1
F-actin/Tm/Tn/S1(+Ca^{2+})	40.9 ± 1.1	38.3 ± 1.8	40.8 ± 2.3	40.7 ± 1.0
F-actin/Tm/Tn/S1(−Ca^{2+})	40.7 ± 1.4	38.4 ± 1.6	40.8 ± 2.2	40.7 ± 1.3

mutant, i.e., closer to F-actin, compared to Cys-282, which exhibited the least efficient FRET (Tables 2 and 3). This result is supported by the finding of Greenfield et al. (40), who showed that the two strands at the very C-terminus of Tm are ill defined and dynamic. It might be expected, therefore, that the average distance between a probe located in this region of Tm and a site on actin would be longer compared to a probe within a more tightly packed α-helical region of Tm, such as that found for Cys-206 and Cys-247.

Regulated thin filaments

The addition of troponin to cTm-F-actin filaments decreased the average distance between BSR and IC5 for some but not all of the loci probed on cTm. For example, FRET efficiency changed from 0.58 to 0.67 for Cys-282 and from 0.66 to 0.72 for Cys-190, whereas smaller differences were found for BSR on Cys-206 and Cys-247 of cTm (Table 2). These results suggested that troponin binding to the thin filament brought about a movement of the C-terminus of cTm (Cys-282) closer to the F-actin, perhaps via an interaction with troponin that reduced the dynamics of the C-terminus. This interpretation would be consistent with a study that showed cardiac troponin T engages in specific interactions with residues at the C-terminus of Tm (41).

Fluorescence anisotropy of BSR-Tm

The relatively high value of the steady-state fluorescence emission anisotropy value of BSR-cross-linked cTm in high salt at room temperature ($r = 0.277$ at 580 nm) suggested that local motions of the donor probe were constrained by tethering. The corresponding values for BSR-labeled cTm mutants varied only slightly around this value, as shown in Table 4. This property is useful for FRET-based analyses of cTm dynamics within the thin filament, since any change in FRET efficiency would more likely reflect movements of the cTm molecule as a whole, rather than independent, local motions of the donor probe. This property was not apparent for probes used in earlier FRET analyses (17–20). Evidence to support this conclusion was obtained through measurements of the steady-state anisotropy of BSR-cTm within reconstituted thin filaments. Thus, despite the significantly larger hydrodynamic volume of the thin filament complex compared to BSR-cTm alone, the anisotropy of the BSR probe increased only slightly to 0.305. This result suggested that BSR emission is not sensitive to any tumbling motions of cTm or from those of the larger thin filament complex. Together, these studies suggested that any change in the anisotropy value of BSR-cTm within the thin filament must reflect a change in the amplitude of orthogonal movements of the entire cTm molecule with respect to the filament axis, as illustrated in Fig. 4.

Movements of tropomyosin in response to Ca^{2+} and myosin S1 binding to the thin filament

The value of FRET efficiency between BSR located on four different sites of cTm and IC5 stoichiometrically attached to F-actin within fully regulated thin filaments was nearly identical between the blocked state and the Ca^{2+}-bound closed state (Table 2). However, the same loci exhibited significant changes in FRET efficiency in response to stoichiometric binding of myosin S1. Analyses of these data showed that the distance between the BSR and IC5 FRET pair decreased at all four loci on cTm (Cys-190, Cys-206, Cys-247, and Cys-282; Table 3). This result supported the finding of Craig and Lehman (15) that the position of the Tm molecule on thin filaments saturated with cross-bridges was different and more defined compared to that found in the Ca^{2+}-activated closed state. The change in distance revealed by our FRET studies was smaller than that deduced from our examination of distances derived from the electron microscopy figures in Craig and Lehman (15), although this was

TABLE 4 Anisotropy of BSR-labeled wild-type cTm and cTm single-cysteine mutants in buffer and within thin filaments

	Tm190C	TmS206C	TmT247C	TmT282C
Tm in buffer	0.277 ± 0.008	0.282 ± 0.009	0.275 ± 0.007	0.273 ± 0.008
F-actin/Tm/Tn(−Ca^{2+})	0.305 ± 0.011	0.316 ± 0.011	0.292 ± 0.010	0.295 ± 0.008
F-actin/Tm/Tn(+Ca^{2+})	0.304 ± 0.011	0.319 ± 0.010	0.303 ± 0.032	0.288 ± 0.007
F-actin/Tm/Tn/S1(+Ca^{2+})	0.313 ± 0.010	0.332 ± 0.009	0.322 ± 0.034	0.326 ± 0.008

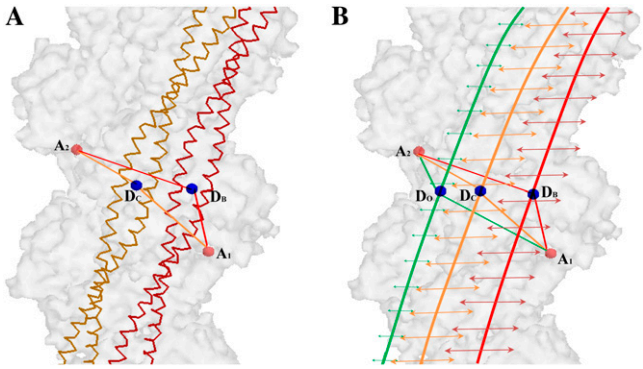

FIGURE 4 A modified three-state model of Tm on the thin filament. (*A*) According to the three-state model (16), the binding of Ca^{2+} to the thin filament triggers a movement of Tm from the blocked state (*red*) to the closed state (*orange*). This should lead to a movement of the donor probe (*purple*) on Tm from D_B to D_C. However, this movement away from acceptor A_1 and toward A_2 made FRET efficiency very insensitive to position change of the Tm. (*B*) Tm exhibited some dynamics orthogonal to the filament axis at the blocked state (*red*) and closed state (*orange*) but was ''frozen'' in the open state (*green*). The structure of the Tm-actin complex is adapted from a published model of the thin filament (16). The diagrams of molecular models were prepared using Protein Explorer 2.80 (48).

expected given our requirement to average FRET over multiple acceptor loci. Since these FRET studies revealed an S1-mediated movement for all four donor sites toward the IC5 acceptor on actin, we suggest that this functional movement involves the entire C-terminal region of cTm, if not the entire cTm molecule. This conclusion is supported by a multisite anisotropy study of BSR-cTm in functional thin filaments, which showed that S1-binding increased the steady-state anisotropy value to a remarkably high value for all four sites on cTm (Table 4). These results suggested that lateral movements of the BSR-cTm molecule on the thin filament were severely hindered by the S1-binding probe, as illustrated in Fig. 4.

Stabilization of the active state by S1 binding was shown to require a higher bound S1/actin ratio in the absence of Ca^{2+} than in the presence of saturating Ca^{2+} (42). To determine whether the movements of cTm exhibited similar behavior, FRET efficiency was measured between Cys-206 or Cys-247 on cTm and Cys-374 on actin, as these pairs exhibited the largest changes in FRET efficiency on S1 binding. The results, presented in Fig. 5, *A* and *B*, showed that the change in FRET efficiency for these D-A pairs followed the typical activation profile by S1. Complete activation in the absence of Ca^{2+} required ~1:1 binding of S1 to actin, whereas activation at saturating Ca^{2+} required ~50% occupancy with S1. This result is very similar to that obtained by the pyrene excimer study in the same condition (in the absence of nucleotide; 11). Thus, activation by S1 binding was normal with this donor/acceptor pair.

Although Ca^{2+} binding to the thin filament did not result in any significant change in FRET efficiency, such a change was

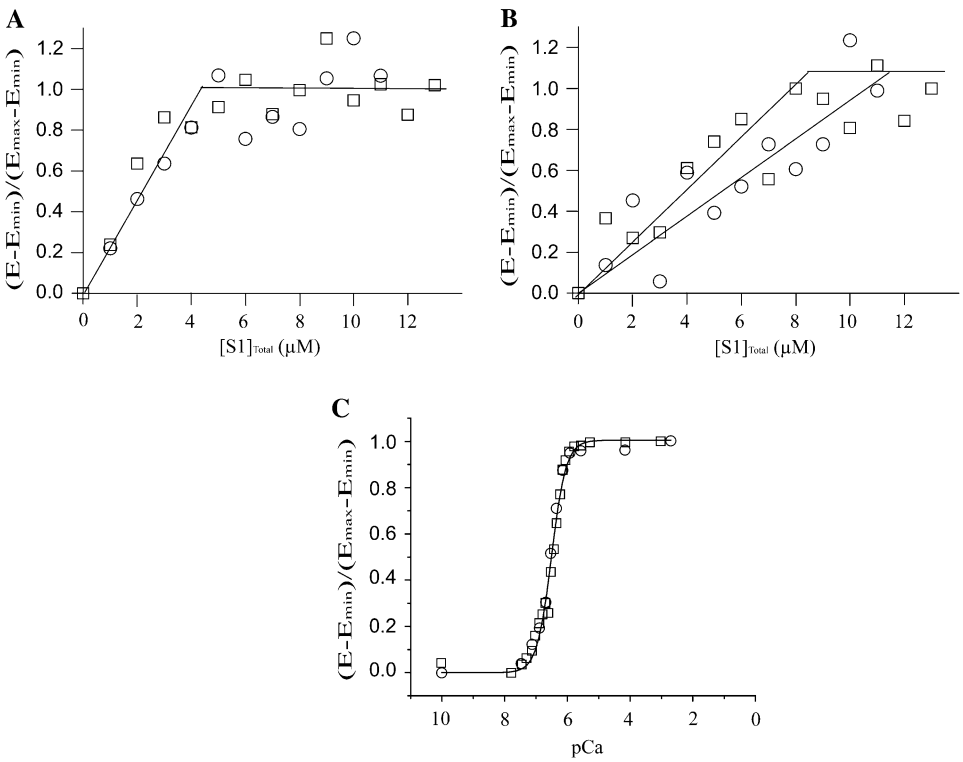

FIGURE 5 FRET efficiency between fluorescein-labeled Tm mutants and TMR-labeled actin in the thin filament titrated with S1 at high calcium (*A*) and at low calcium (*B*). A 10 μM thin filament preparation was titrated with S1 in the presence of 0.1 mM Ca^{2+} (*A*) or 1 mM EGTA (*B*), and the FRET efficiency was normalized as $(E - E_{min})/(E_{max} - E_{min})$. The mutant Tm206C was shown as squares, and the mutant Tm247C was shown as circles. The break point of the curves in *A* and *B* was estimated from a series of linear least squares fits of the data beginning from [S1] = 0 to and ending at different points. (*C*) The fluorescence of fluorescein-labeled Tm mutants TmS206C (*squares*) and TmT247C (*circles*) in the presence of 10 μM TMR-labeled actin in the thin filament titrated with Ca^{2+} in the presence of 2 μM S1. The FRET efficiency was normalized as $(E - E_{min})/(E_{max} - E_{min})$. The following equation was fitted to the data: $(E - E_{min})/(E_{max} - E_{min}) = [Ca^{2+}]^n/(K^n + [Ca^{2+}]^n)$. The Hill constant, n, was 1.9. The concentration of calcium giving 50% of the maximum fluorescence change, K, was 3×10^{-7}M.

demonstrated when the thin filament was partially saturated with S1. From a comparison of Fig. 5, *A* and *B*, one would predict an increase in the normalized FRET efficiency upon binding to Ca^{2+}, provided that the S1/actin ratio was between ~0.2 and 0.8. The normalized change in FRET efficiency as a function of pCa when 20% of the actin bound to S1 in the absence of ATP was measured and plotted in Fig. 5 *C*. As expected, FRET efficiency changed as the pCa was varied. The Hill coefficient was calculated as 1.9 and the pCa_{50} was 6.5. These values are similar to those obtained with dansylaziridine-labeled troponin C (43).

Comparison with previous FRET studies on tropomyosin dynamics

Earlier steady-state FRET studies failed to detect any significant Ca^{2+}-triggered movements of Tm within the thin filament (17,18,20). A Ca^{2+}-induced change in the locus of Tm on actin was reported by Bacchiocchi and Lehrer (19) using frequency domain measurements of the decay of a Dansyl donor to a highly immobile TMR-phalloidin on F-actin (25). In that study, the χ^2 value obtained for the decay of the excited-state donor in the absence of acceptor was best described by three exponentials, although the χ^2 value from the same analysis was not reported for Dansyl in the presence of acceptor. Instead, a model-dependent analysis was employed that involved finding the best fit to the raw phase/modulation data for the $\pm Ca^{2+}$ conditions by varying the relative coordinates of Tm with respect to actin (19).

This analysis suggested that Tm undergoes a 17° azimuthally Ca^{2+} movement on the filament with respect to actin, although the significance of this result must be considered in light of the large errors in the calculated angles, i.e., $-14° \pm 12°$ in the absence of Ca^{2+} versus $3° \pm 13°$ in the presence of Ca^{2+}; and although the χ^2 value for the $+Ca^{2+}$ FRET condition was almost twice as high as the $-Ca^{2+}$ condition (19), the additional uncertainty in the measurement by assuming a value of κ^2 for the highly immobile TMR-phalloidin acceptor probe (25) was not evaluated. Nonetheless, if the general conclusion from this study was correct, it could also be argued that the very large uncertainty in the calculated azimuthal angles could reflect a distribution of Tm loci on the thin filament. If so, the loci of Tm in the blocked and closed states of the thin filament might be expected to overlap, at least as far as the resolution of the FRET technique is concerned, a conclusion that is consistent with the measurements and analyses presented in this study.

One could also argue that the failure of earlier FRET studies to detect Ca^{2+}-mediated movements of Tm was due, in part, to the employment of ill-defined donor probes on Tm (17–20) and/or the use of a substoichiometric level of Tm in the thin filament (19) and/or overlapping loci of the probe on Tm in the blocked and closed states. These complicating issues were resolved in this study through the use of a novel labeling approach that introduced a single tethered donor probe between in-register cysteine residues within a single, functional cTm dimer.

It could equally be argued that the movement of Tm on the thin filament in response to Ca^{2+} binding falls below the resolution of the FRET technique; indeed the sensitivity of FRET measurements to azimuthal movements (illustrated in Fig. 4 *A*) is reduced by the presence of multiple acceptor loci. However, given the large number of different types of donor and acceptor probes that have been used in earlier FRET studies and their placements at significantly different loci on Tm and actin, it seems unlikely that the multiple acceptor effect could account for the uniform failure to observe any Ca^{2+}-mediated movements of Tm on the thin filament. Interestingly a luminescence resonance energy transfer study that used terbium ion as an isotropic donor (44) labeled on one Tm dimer and TMR as an acceptor probe on the Tm dimer across the actin filament to avoid the multiple acceptor problems also failed to detect Ca^{2+}-induced movement of Tm on the thin filament.

Conclusions drawn from this study suggest that the insensitivity of FRET to sense Ca^{2+}-induced movements of cTm resulted from thermally mediated, orthogonal fluctuations of cTm with respect to the filament axis in the blocked and/or closed state that lead to an overlap in the position of donor probe between these two states. Indirect evidence that the Tm molecule is flexible on the thin filament is suggested from its weak binding to F-actin when assayed at substoichiometric levels (45). The stronger binding of Tm to the thin filament, seen under stoichiometric-binding conditions, involves overlapping interactions of Tm at their N- and C-termini as well as those at the Tm-Tn interface. On the other hand, stretches of the Tm molecule away from troponin engage in only weak and transient interactions with actin that are likely influenced by thermal fluctuations.

Evidence in support of the flexible nature of Tm on the thin filament comes from an NMR study (46), where it was shown that specific repeats in the Tm molecule are capable of undergoing folding-unfolding transitions, and an electron paramagnetic resonance study (47), where it was shown that Tm is flexible and disordered in skeletal thin filament. Thus, if cTm exhibited thermally driven fluctuations in both the blocked and closed states then the average separation of the BSR probe would be reduced, limiting the effectiveness of FRET to detect a Ca^{2+}-mediated movement. On the other hand, the binding of S1 to Ca^{2+}-bound thin filaments was accompanied by a significant change in FRET efficiency and anisotropy, which we argued resulted from a significant movement of cTm on the thin filament (Table 4). The S1-mediated movement of cTm was mapped to all four loci on the C-terminal half of cTm (Cys-190 to Cys-282), which suggested a movement of the entire cTm molecule on the thin filament. The S1-mediated movement of cTm to the open state was shown to be highly cooperative and exhibited a similar dependence as the Ca^{2+}/S1-mediated activation of the S1-ATPase. We therefore suggest that the S1-mediated

structural movement of cTm is a consequence of, and is directly coupled to, the activation of the thin filament.

We thank Dr. Kenneth C. Holmes for providing the curved tropomyosin coordinates model.

This work was supported by the National Institutes of Health (HLO69970 awarded to GM and AR40540 to JMC).

REFERENCES

1. Huxley, H. E. 1972. Structural changes in the actin- and myosin-containing filaments during contraction. *Cold Spring Harb. Symp. Quant. Biol.* 37:361–376.
2. Parry, D. A., and J. M. Squire. 1973. Structural role of tropomyosin in muscle regulation: analysis of the x-ray diffraction patterns from relaxed and contracting muscles. *J. Mol. Biol.* 75:33–55.
3. Chalovich, J. M., P. B. Chock, and E. Eisenberg. 1981. Mechanism of action of troponin-tropomyosin. Inhibition of actomyosin ATPase activity without inhibition of myosin binding to actin. *J. Biol. Chem.* 256:575–578.
4. Chalovich, J. M., and E. Eisenberg. 1982. Inhibition of actomyosin ATPase activity by troponin-tropomyosin without blocking the binding of myosin to actin. *J. Biol. Chem.* 257:2432–2437.
5. Chalovich, J. M. 1992. Actin mediated regulation of muscle contraction. *Pharmacol. Ther.* 55:95–148.
6. Hill, T. L., E. Eisenberg, and L. Greene. 1980. Theoretical model for the cooperative equilibrium binding of myosin subfragment 1 to the actin-troponin-tropomyosin complex. *Proc. Natl. Acad. Sci. USA.* 77: 3186–3190.
7. Hill, T. L. 1983. Two elementary models for the regulation of skeletal muscle contraction by calcium. *Biophys. J.* 44:383–396.
8. Lehrer, S. S., and E. P. Morris. 1982. Dual effects of tropomyosin and troponin-tropomyosin on actomyosin subfragment 1 ATPase. *J. Biol. Chem.* 257:8073–8080.
9. Lehrer, S. S. 1994. The regulatory switch of the muscle thin filament: Ca^{2+} or myosin heads? *J. Muscle Res. Cell Motil.* 15:232–236.
10. Maytum, R., S. S. Lehrer, and M. A. Geeves. 1999. Cooperativity and switching within the three-state model of muscle regulation. *Biochemistry.* 38:1102–1110.
11. Ishii, Y., and S. S. Lehrer. 1987. Fluorescence probe studies of the state of tropomyosin in reconstituted muscle thin filaments. *Biochemistry.* 26:4922–4925.
12. Swartz, D. R., R. L. Moss, and M. L. Greaser. 1996. Calcium alone does not fully activate the thin filament for S1 binding to rigor myofibrils. *Biophys. J.* 71:1891–1904.
13. McKillop, D. F., and M. A. Geeves. 1993. Regulation of the interaction between actin and myosin subfragment 1: evidence for three states of the thin filament. *Biophys. J.* 65:693–701.
14. Xu, C., R. Craig, L. S. Tobacman, R. Horowitz, and W. Lehman. 1999. Tropomyosin positions in regulated thin filaments revealed by cryoelectron microscopy. *Biophys. J.* 77:985–992.
15. Craig, R., and W. Lehman. 2001. Crossbridge and tropomyosin positions observed in native, interacting thick and thin filaments. *J. Mol. Biol.* 311:1027–1036.
16. Pirani, A., M. V. Vinogradova, P. M. Curmi, W. A. King, R. J. Fletterick, R. Craig, L. S. Tobacman, C. Xu, V. Hatch, and W. Lehman. 2006. An atomic model of the thin filament in the relaxed and Ca^{2+}-activated states. *J. Mol. Biol.* 357:707–717.
17. Tao, T., M. Lamkin, and S. S. Lehrer. 1983. Excitation energy transfer studies of the proximity between tropomyosin and actin in reconstituted skeletal muscle thin filaments. *Biochemistry.* 22:3059–3066.
18. Miki, M., T. Miura, K. Sano, H. Kimura, H. Kondo, H. Ishida, and Y. Maéda. 1998. Fluorescence resonance energy transfer between points on tropomyosin and actin in skeletal muscle thin filaments: does tropomyosin move? *J. Biochem.* 123:1104–1111.
19. Bacchiocchi, C., and S. S. Lehrer. 2002. Ca^{2+}-induced movement of tropomyosin in skeletal muscle thin filaments observed by multi-site FRET. *Biophys. J.* 82:1524–1536.
20. Miki, M., H. Hai, K. Saeki, Y. Shitaka, K. Sano, Y. Maéda, and T. Wakabayashi. 2004. Fluorescence resonance energy transfer between points on actin and the C-terminal region of tropomyosin in skeletal muscle thin filaments. *J. Biochem.* (*Tokyo*). 136:39–47.
21. Spudich, J. A., and S. Watt. 1971. The regulation of rabbit skeletal muscle contraction. I. Biochemical studies of the interaction of the tropomyosin-troponin complex with actin and the proteolytic fragments of myosin. *J. Biol. Chem.* 246:4866–4871.
22. Lehrer, S. S., and G. Kerwar. 1972. Intrinsic fluorescence of actin. *Biochemistry.* 11:1211–1217.
23. Potter, J. D. 1982. Preparation of troponin and its subunits. *Methods. Enzymol.* 85:241–263.
24. Weeds, A. G., and R. S. Taylor. 1975. Separation of subfragment-1 isoenzymes from rabbit skeletal muscle myosin. *Nature.* 257:54–56.
25. Heidecker, M., Y. Yan-Marriott, and G. Marriott. 1995. Proximity relationships and structural dynamics of the phalloidin binding site of actin filaments in solution and on single actin filaments on heavy meromyosin. *Biochemistry.* 34:11017–11025.
26. Marriott, G., K. Zechel, and T. M. Jovin. 1988. Spectroscopic and functional characterization of an environmentally sensitive fluorescent actin conjugate. *Biochemistry.* 27:6214–6220.
27. Kodama, T., K. Fukui, and K. Kometani. 1986. The initial phosphate burst in ATP hydrolysis by myosin and subfragment-1 as studied by a modified malachite green method for determination of inorganic phosphate. *J. Biochem.* (*Tokyo*). 99:1465–1472.
28. Förster, Th. 1948. Intermolecular energy migration and fluorescence. *Annalen der Physik.* 2:55–75.
29. Fairclough, R. H., and C. R. Cantor. 1978. The use of singlet-singlet energy transfer to study macromolecular assemblies. *Methods Enzymol.* 48:347–379.
30. Karstens, T., and K. Kobs. 1980. Rhodamine B and rhodamine 101 as reference substances for fluorescence quantum yield measurements. *J. Phys. Chem.* 84:1871–1872.
31. Whitby, F. G., and G. N. Phillips Jr. 2000. Crystal structure of tropomyosin at 7 Angstroms resolution . *Proteins.* 38:49–59.
32. Ito, K., X. Liu, E. Katayama, and T. Q. P. Uyeda. 1999. Cooperativity between two heads of dictyostelium myosin II in in vitro motility and ATP hydrolysis. *Biophys. J.* 76:985–992.
33. Prassler, J., A. Murr, S. Stocker, J. Faix, and G. Marriott. 1998. Molecular and cellular characterization of a LIM-domain protein from the cytoskeleton of Dictyostelium. *Mol. Biol. Cell.* 9:554–559.
34. Lakowicz, J. R. 2006. Principles of Fluorescence Spectroscopy, 3rd ed. Springer, New York.
35. Dale, R. E., and J. Eisinger. 1975. Polarized excitation energy transfer. *In* Biochemical Fluorescence, Concepts, Vol. 1. R. F. Chen and H. Edelhoch, editors. Marcel Dekker, New York. 115–284.
36. Dale, R. E., and J. Eisinger. 1974. Intramolecular distances determined by energy transfer: dependence on orientation freedom of donor and acceptor. *Biopolymers.* 13:1573–1605.
37. Poole, K. J. V., M. Lorenz, G. Evans, G. Rosenbaum, A. Pirani, R. Craig, L. S. Tobacman, W. Lehman, and K. C. Holmes. 2006. A comparison of muscle thin filament models obtained from electron microscopy reconstructions and low-angle x-ray fibre diagrams from non-overlap muscle. *J. Struct. Biol.* 155:273–284.
38. VanBeek, D. B., M. C. Zwier, J. M. Shorb, and B. P. Krueger. 2007. Fretting about FRET: correlation between κ and R. *Biophys. J.* 92:4168–4178.
39. Yan, Y., and G. Marriott. 2003. FRET image microscopy and fluorescence polarization image microscopy. *Methods Enzymol.* 36:560–582.
40. Greenfield, N. J., T. Palm, and S. E. Hitchcock-DeGregori. 2002. Structure and interactions of the carboxyl terminus of striated muscle alpha-tropomyosin: it is important to be flexible. *Biophys. J.* 83:2754–2766.

41. Ishii, Y., and S. S. Lehrer. 1991. Two-site attachment of troponin to pyrene-labeled tropomyosin. *J. Biol. Chem.* 266:6894–6903.

42. Greene, L. E., and E. Eisenberg. 1988. Relationship between regulated actomyosin ATPase activity and cooperative binding of myosin to regulated actin. *Cell Biophys.* 12:59–71.

43. Grabarek, Z., J. Grabarek, P. C. Leavis, and J. Gergely. 1983. Cooperative binding to the Ca^{2+}-specific sites of troponin C in regulated actin and actomyosin. *J. Biol. Chem.* 258:14098–14102.

44. Chen, Y., and S. S. Lehrer. 2004. Distances between tropomyosin sites across the muscle thin filament using luminescence resonance energy transfer: evidence for tropomyosin flexibility. *Biochemistry.* 43:11491–11499.

45. Hill, L. E., J. P. Mehegan, C. A. Butters, and L. S. Tobacman. 1992. Analysis of troponin-tropomyosin binding to actin. Troponin does not promote interactions between tropomyosin molecules. *J. Biol. Chem.* 267:16106–16113.

46. Singh, A., and S. E. Hitchcock-DeGregori. 2003. Local destabilization of the tropomyosin coiled coil gives the molecular flexibility required for actin binding. *Biochemistry.* 42:14114–14121.

47. Szczesna, D., and P. G. Fajer. 1995. The tropomyosin domain is flexible and disordered in reconstituted thin filaments. *Biochemistry.* 34:3614–3620.

48. Martz, E. 2007. FrontDoor to Protein Explorer 2.80. http://www.proteinexplorer.org.